

# **Status of GEp-III/GEp-2 $\gamma$ Archival Results/Publication**

Andrew Puckett

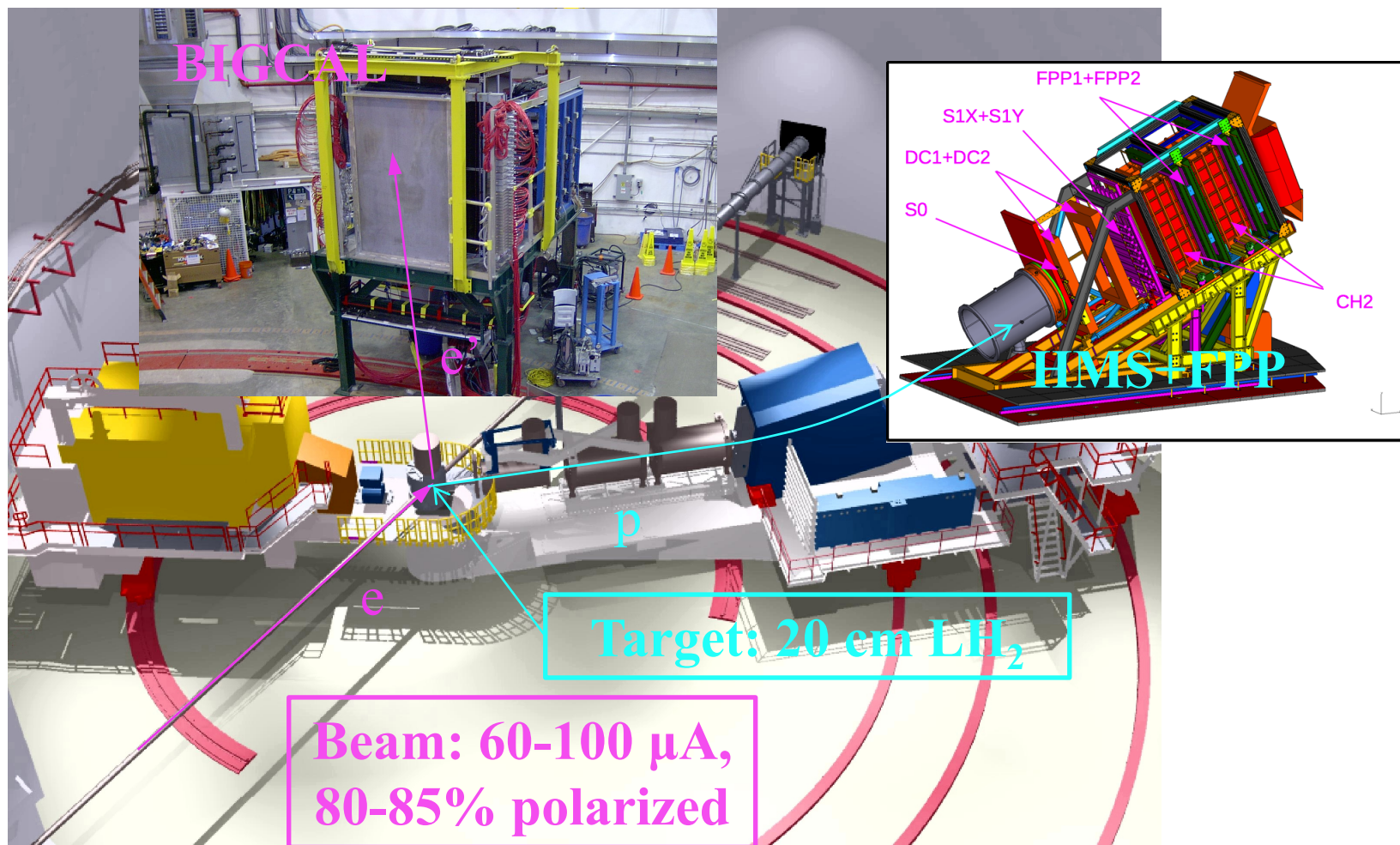
University of Connecticut

On behalf of the GEp-III Collaboration

# Outline

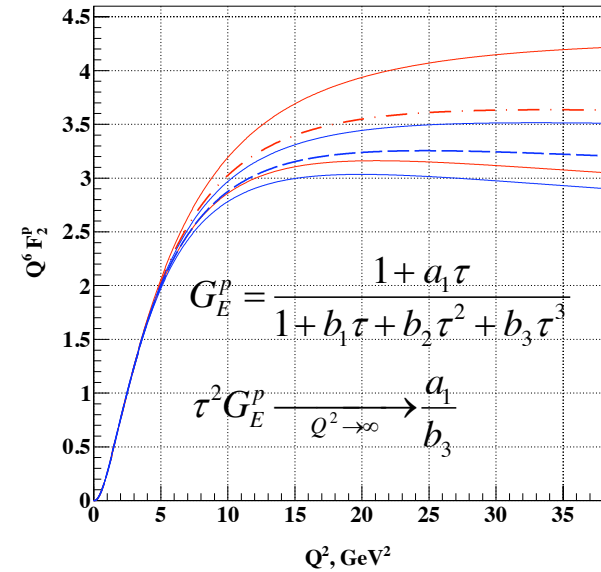
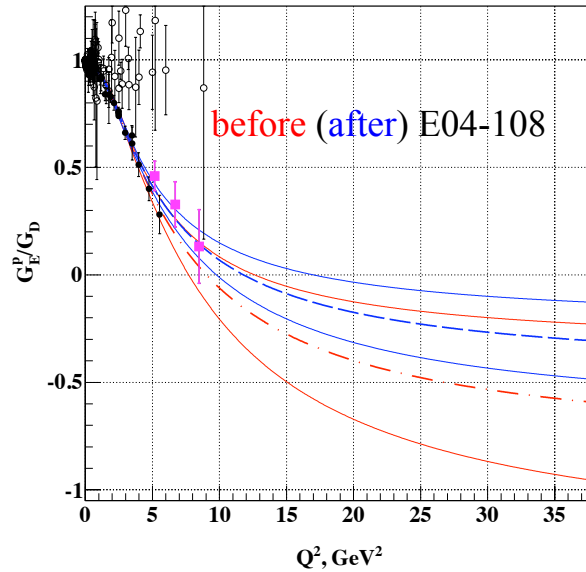
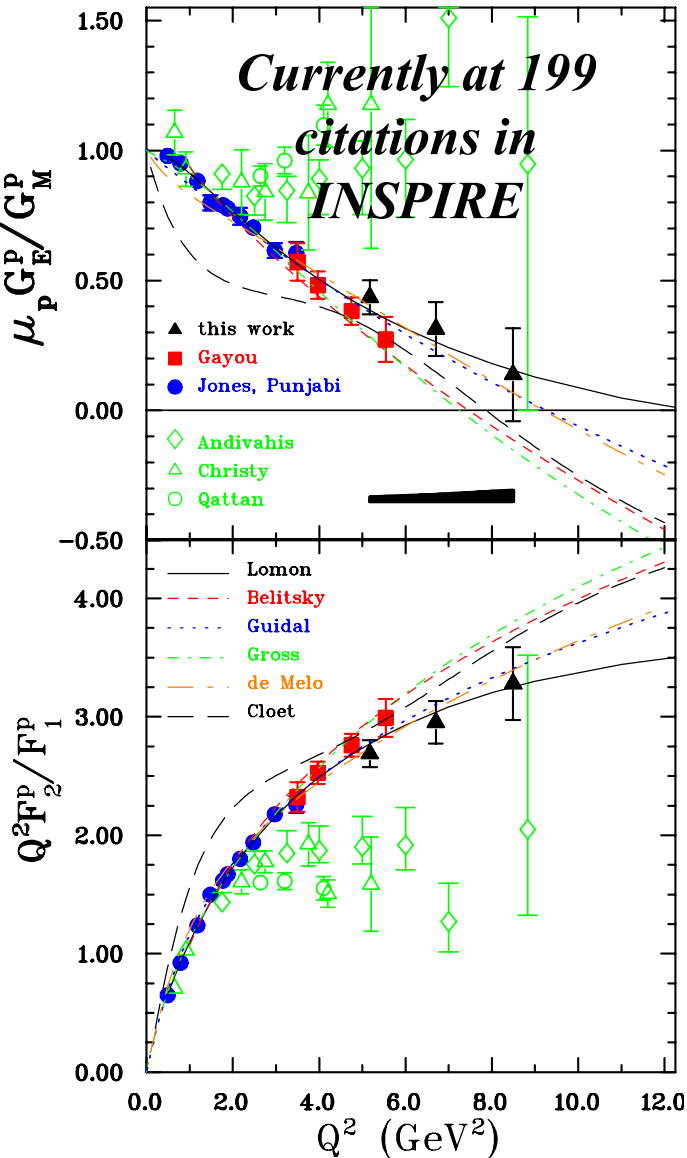
- Review of GEp-III/GEp- $2\gamma$  experiments in Hall C at JLab
- Existing publications from Hall C polarization transfer experiments
- Re-analysis of the Hall C data
- *New results from GEp- $2\gamma$  data including unpublished full-acceptance data*
- PRELIMINARY (not for public distribution/discussion/consumption) results of final analysis
- Status of draft PRC publication on combined Hall C GEP measurements

# The GEp-III and GEp-2 $\gamma$ Experiments in Hall C



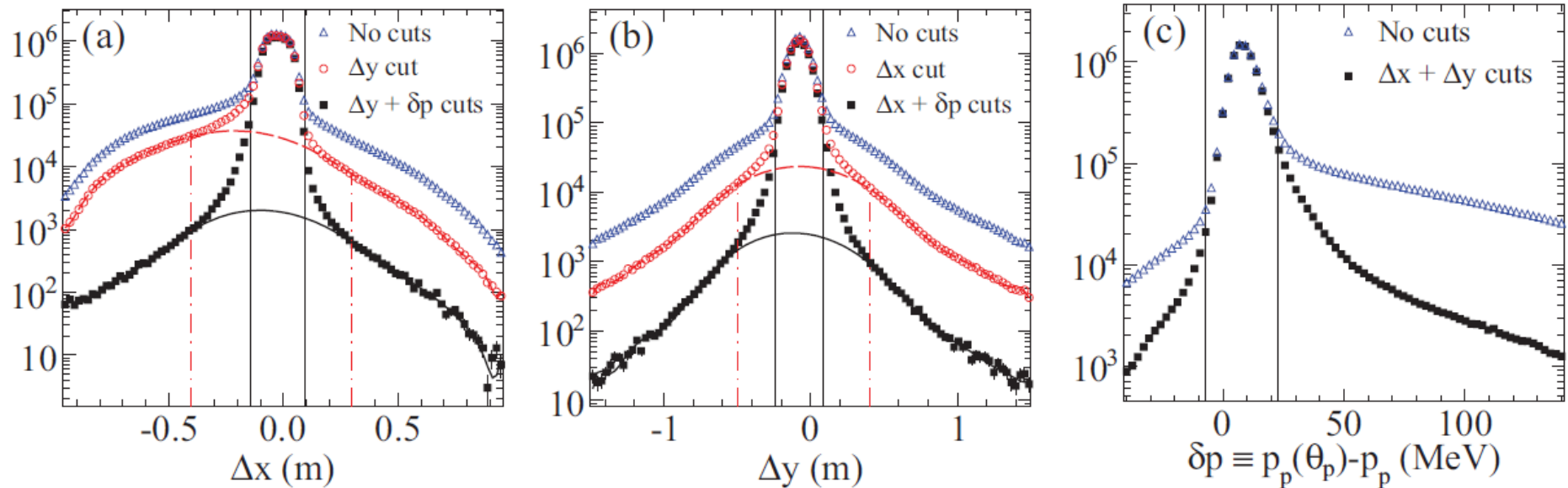
Polarization transfer in  $^1\text{H}(e, e'p)$ . Nominal luminosity  $\sim 4 \times 10^{38}$  Hz/cm<sup>2</sup>

# GEp-III Results: PRL 104, 242301 (2010)



- Increased  $Q^2$  coverage of the data by  $\sim 50\%$
- All three points at least  $1.5\sigma$  above Gayou linear fit to GEp-I/II data:
  - *Possible consistency issue between Halls A/C?*
- Rate of decrease of  $G_{Ep}/G_{Mp}$  slowing down
- Error bars in high- $Q^2$ /asymptotic  $G_{Ep}/F_{2p}$  reduced by  $\sim$ factor of 2 in a global analysis using the Kelly fit.

# GEP-II reanalysis—Elastic event selection

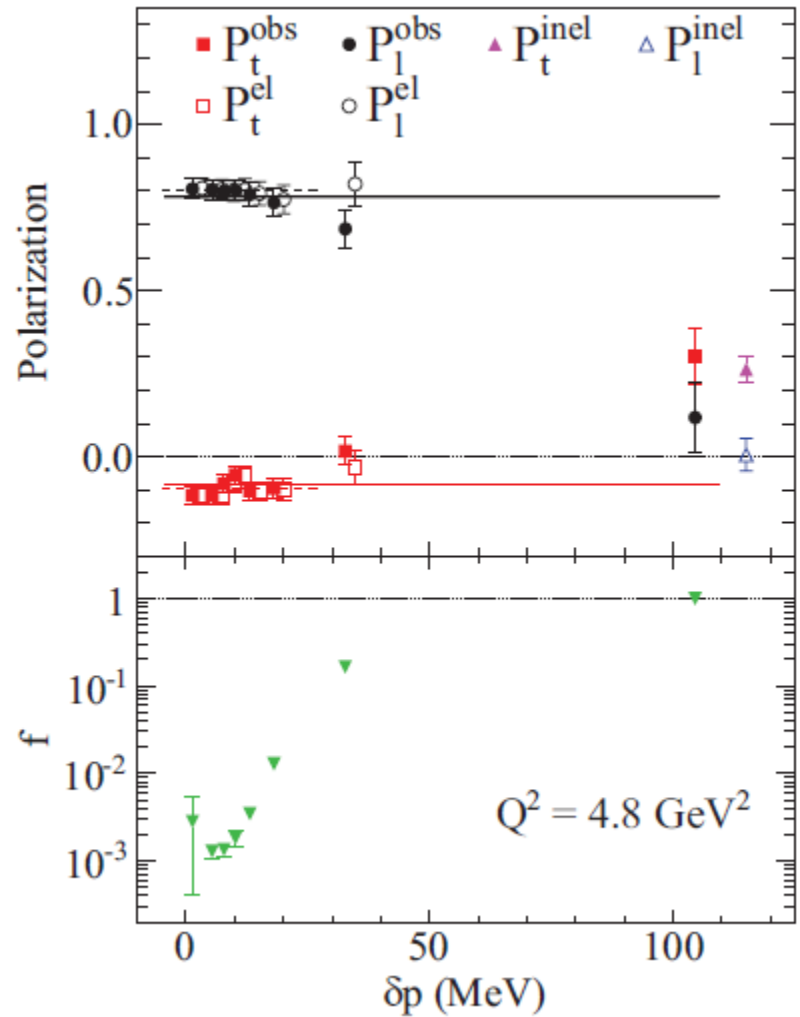
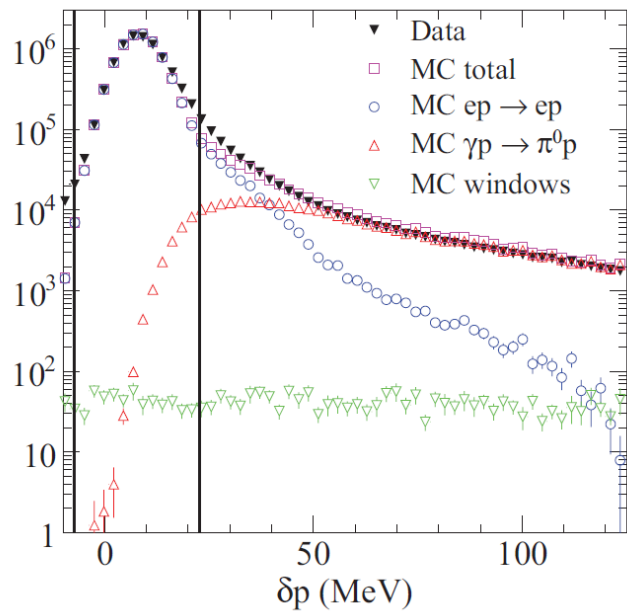


## *Elastic event selection in GEP-II, $Q^2 = 4.8 \text{ GeV}^2$*

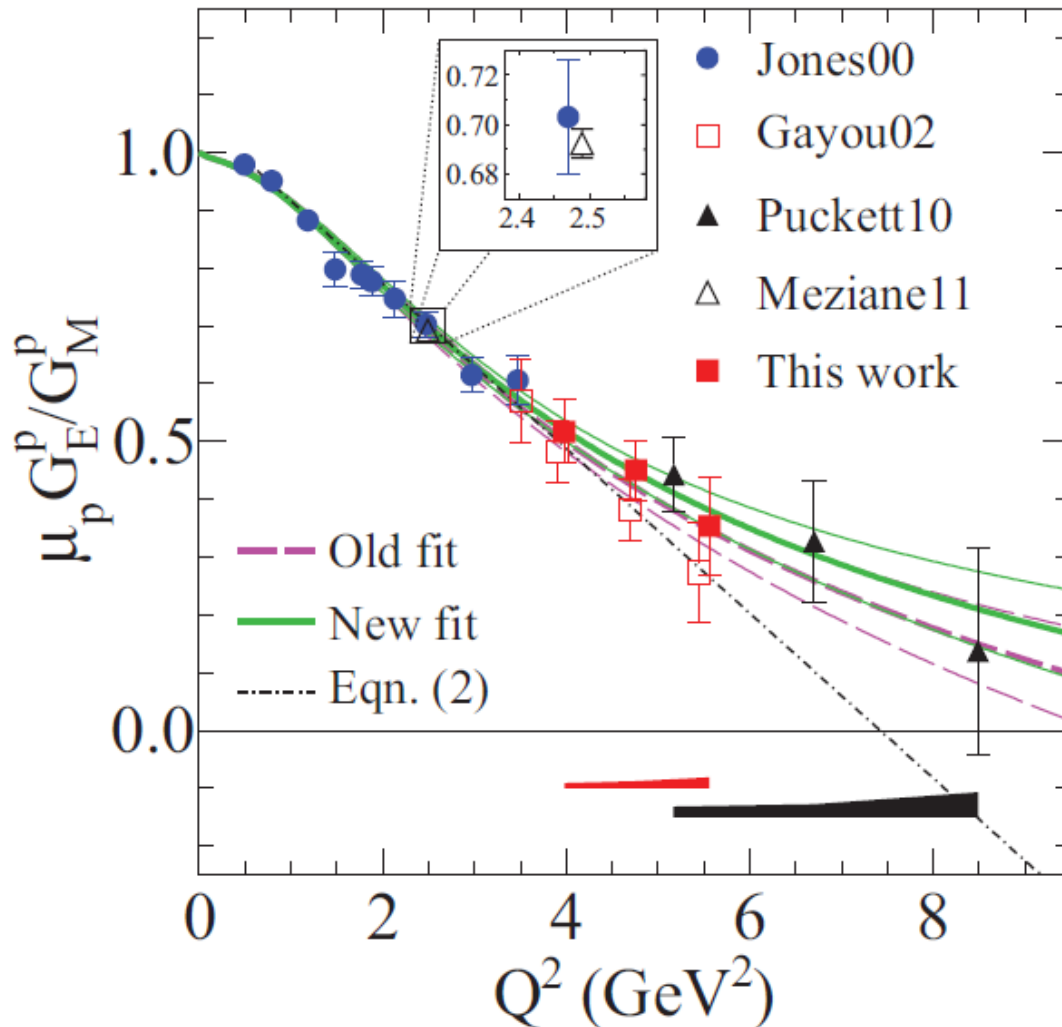
- Elastic event selection in GEP-II: similar to GEP-III but with different dominant sources of resolution
- $\gamma p \rightarrow \pi^0 p$  background led to significant **positive** corrections to R in GEP-III at  $8.5 \text{ GeV}^2$ ; proton  $p(\theta) - p$  cut found crucial, but *no such cut* was applied in original GEP-II analysis
- Even a small contamination can have a large effect on asymmetries!
- Motivated a new analysis of the GEP-II data at  $Q^2 = 4.0, 4.8, 5.6 \text{ GeV}^2$ , for which electrons were also detected by a lead-glass calorimeter as in GEP-III

# Effect of the underestimated background

- Most events outside the elastic peak of  $\delta p = p(\theta) - p$  are background-dominated.
- The observed polarization components evolve from those of the signal to those of the background as  $\delta p$  increases
- Net systematic effect is  $\sim 15\%$  in  $P_T$ , 2% in  $P_L$
- Conclusions borne out by Monte Carlo:



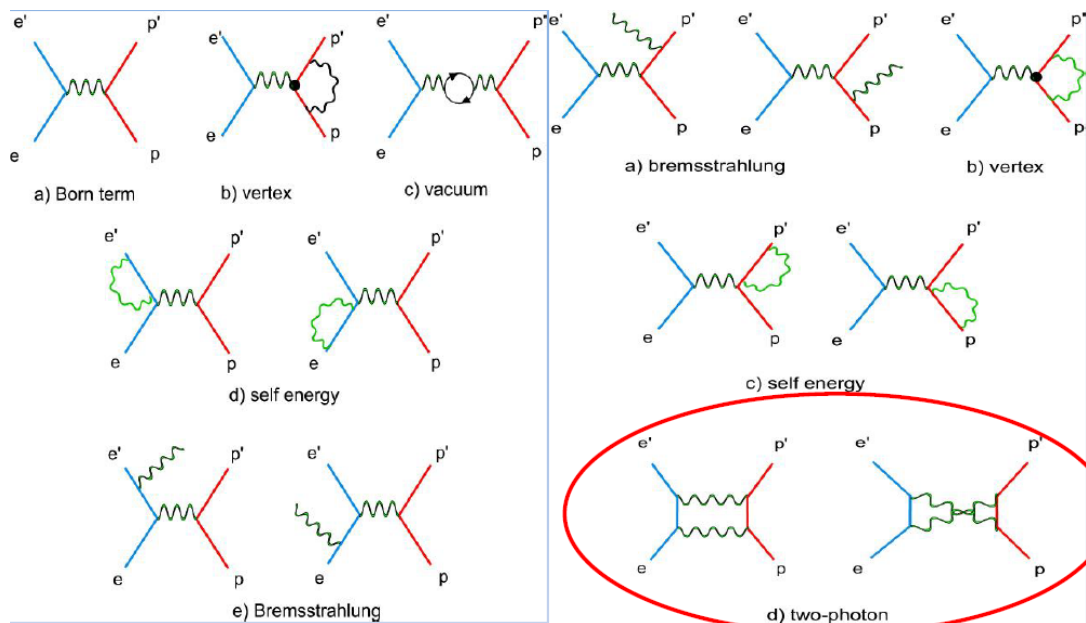
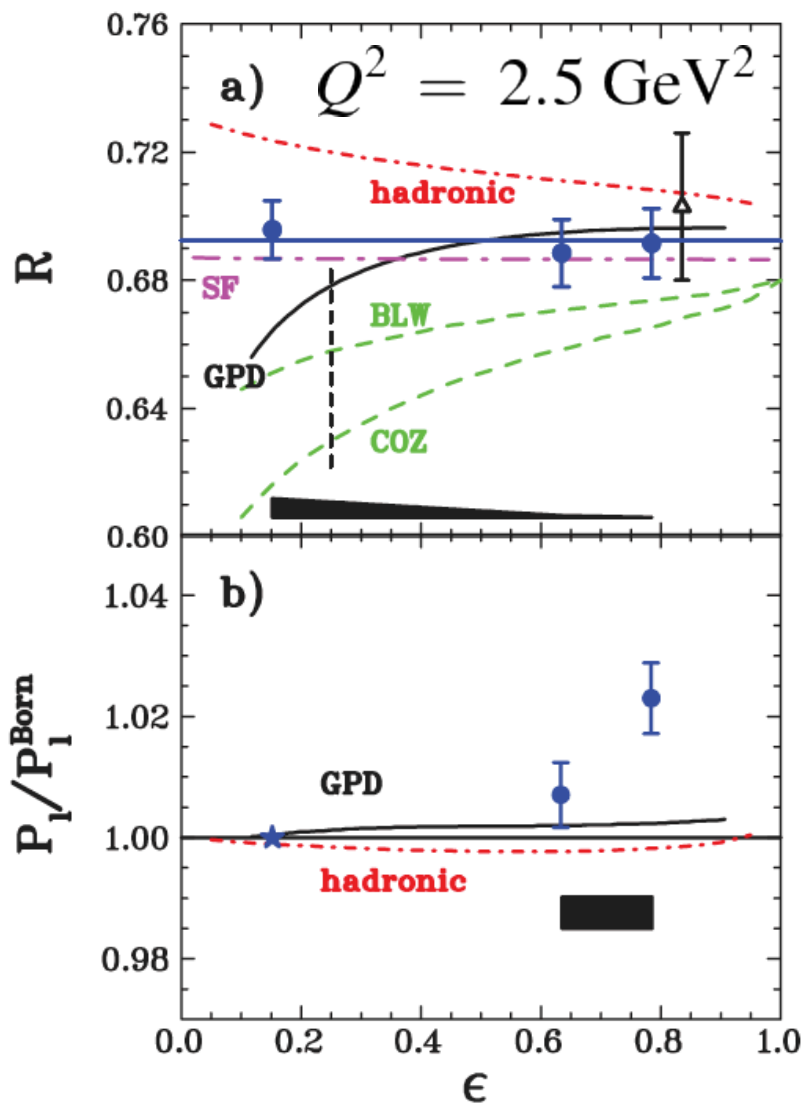
# Final Results of GEp-II



## Summary of results

- Reanalyzed three highest- $Q^2$  points (electron detected in calorimeter)
- Lowest  $Q^2 = 3.5 \text{ GeV}^2$  not reanalyzed (electron detected in HRSR).
- Three highest- $Q^2$  R values systematically increase, by several times the originally quoted systematics.
  - **Increase mainly due to previously underestimated background**
- Addition of  $p(\theta) - p$  cut suppresses background to  $<0.4\%$ , remaining correction and uncertainty small
- Consistency of GEp-I/II/III/ $2\gamma$  data (Hall A vs. Hall C) is now excellent in a wide  $Q^2$  range
- **Updated analysis and results now published in *Phys. Rev. C, PRC 85, 085, 045203***

# GEp-2 $\gamma$ Results: PRL 106, 132501 (2011)



- Results show no  $\epsilon$ -dependence of the ratio  $R$  ( $= \mu_{G_E}/G_M$  in Born approximation) at the 1% level at  $Q^2 = 2.5 \text{ GeV}^2$
- Relative variation of  $P_L/P_L(\text{Born})$  with  $\epsilon$  shows a  $\sim 2\%$  enhancement at large  $\epsilon$  relative to small  $\epsilon$ —not predicted by any model calculations of TPEX (available at the time of publication)

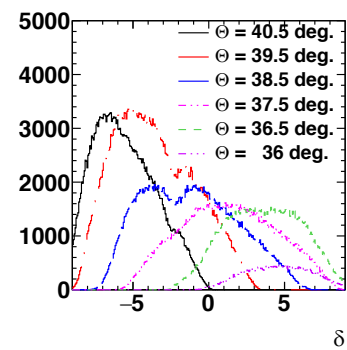
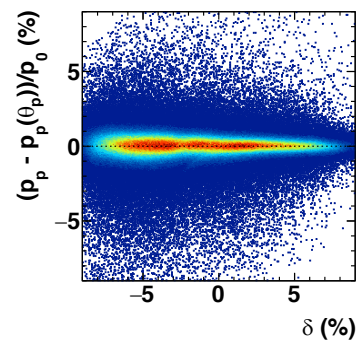
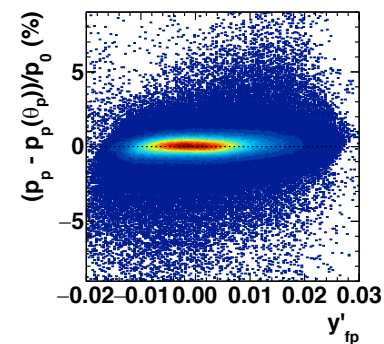
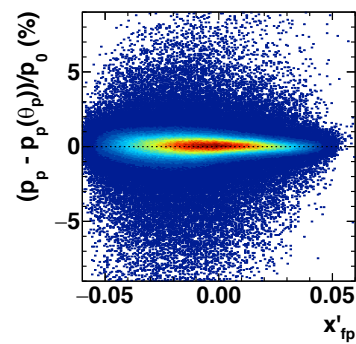
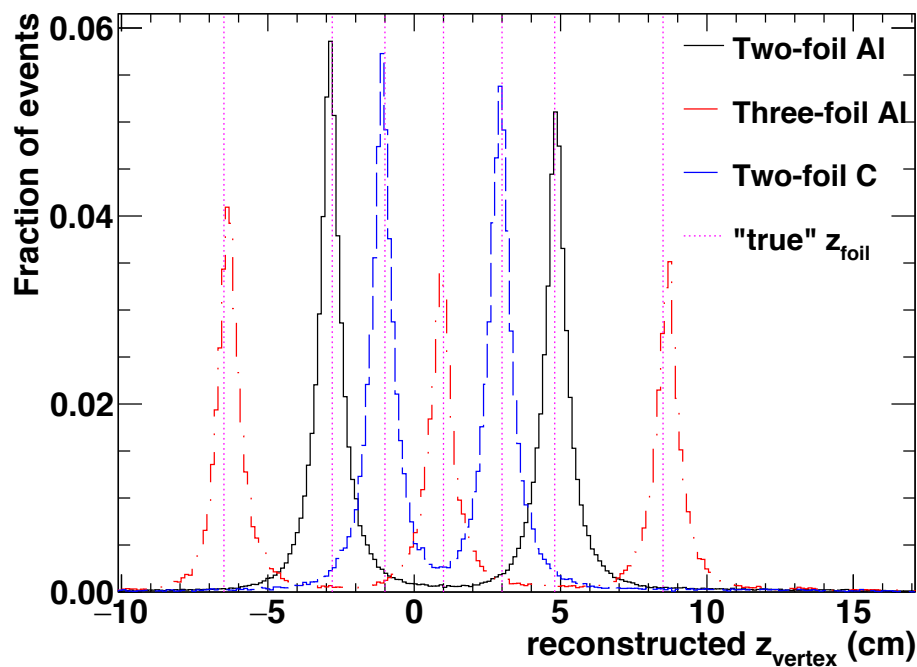
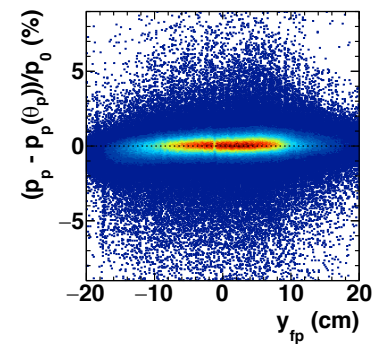
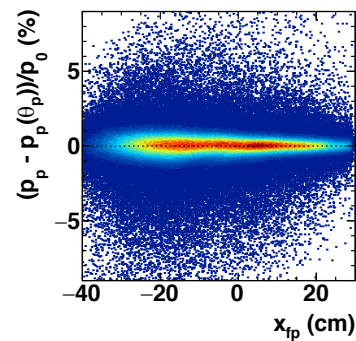
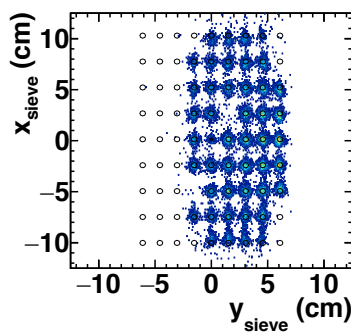
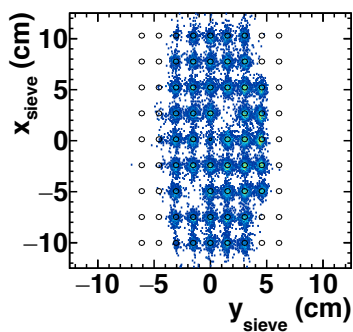
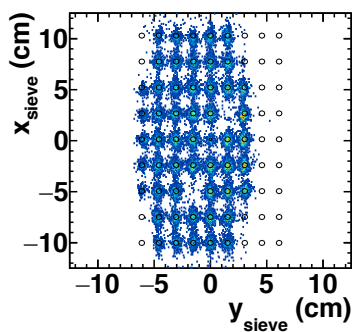
$$P_\ell^{\text{Born}} = \frac{\sqrt{1 - \epsilon^2}}{1 + \frac{\epsilon}{\tau} \left( \frac{G_E}{G_M} \right)^2} \quad R \equiv -\mu_p \sqrt{\frac{\tau(1 + \epsilon)}{2\epsilon}} \frac{P_t}{P_\ell}$$



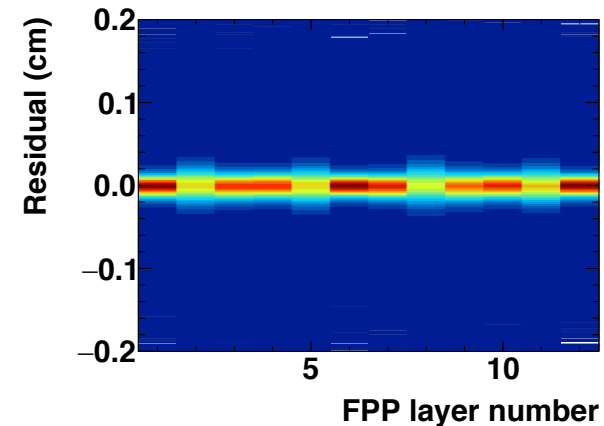
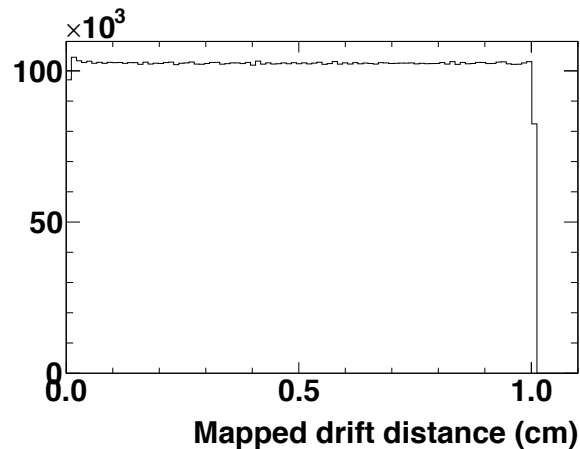
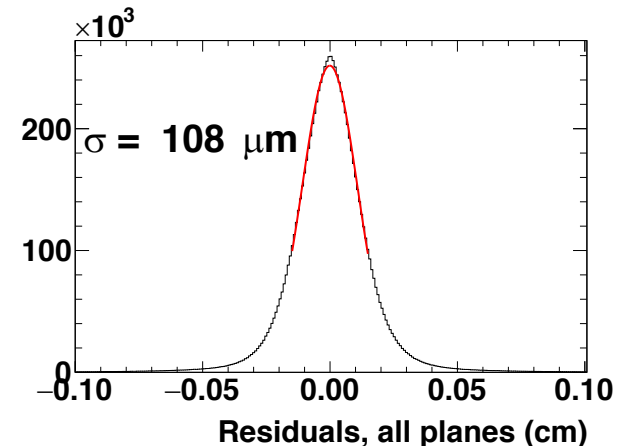
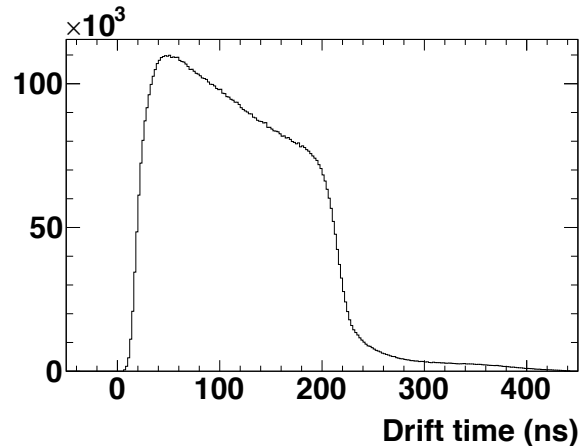
# New/Final analysis of the Hall C data

- Goal: Improve understanding of systematic uncertainties in order to publish full-acceptance results from GEp-2g and final archival results from GEp-2g/GEp-III.
- Major aspects of event reconstruction/calibration revisited:
  - **HMS optics calibration: angle and vertex reconstruction**
  - **HMS and FPP time-to-distance calibration performed run-by-run (and card-by-card for FPP drift chambers)**
  - **Improved FPP-HMS drift chamber alignment from straight-through data**
  - Minor improvements/bug fixes to HMS/FPP tracking algorithms
  - Recalibration of BigCal energy reconstruction for some run ranges with room for improvement
  - Minor improvements to BigCal shower coordinate reconstruction
  - Updated beam position/energy database from EPICS (beam position + raster corrections important for momentum/out-of-plane angle reconstruction)
  - More thorough run-by-run data quality checks; exclusion of runs with significant FPP data quality issues from GEp-2gamma analysis (minimize false asymmetries)
- Major aspects of physics analysis revisited:
  - Use of more efficient variable-width exclusivity cuts to account for variations of the widths of several exclusivity cut variables within the HMS acceptance (compared to fixed-width cuts used in the analysis for PRL publications)
  - Improved “fully differential” description of the analyzing power
  - Understanding of finite-acceptance/bin-centering effects on  $P_T$ ,  $P_L$ ,  $R$

# HMS Optics Calibrations

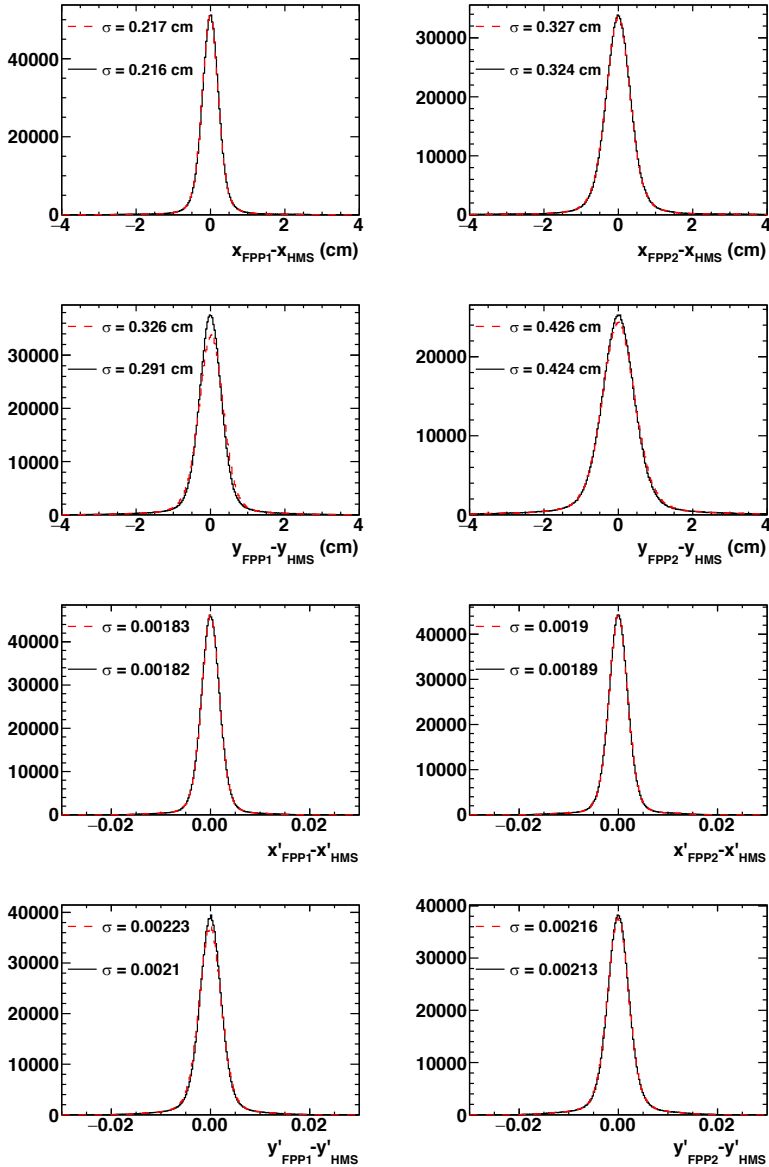


# HMS and FPP drift-map database

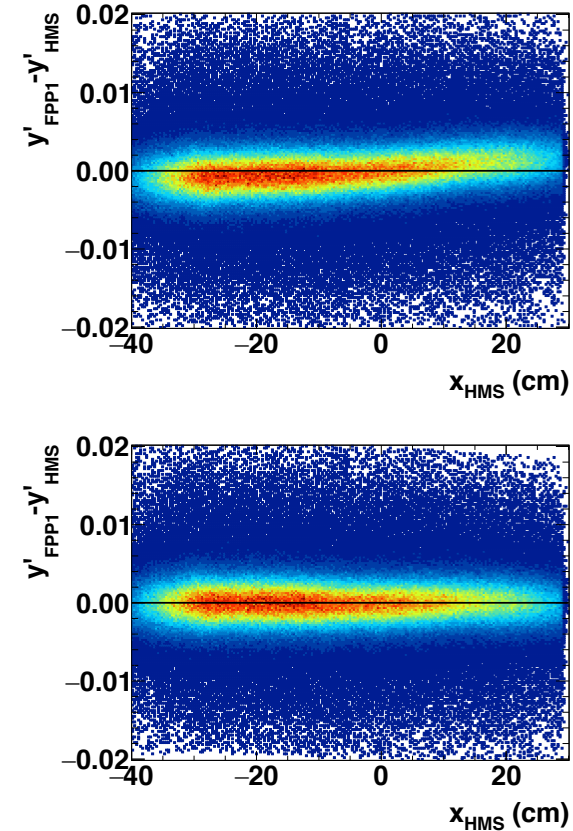


- Left: Example FPP drift time spectrum and mapped uniform drift distance distribution within a cell
- Right: FPP tracking residuals, averaged and by plane number

# FPP alignment

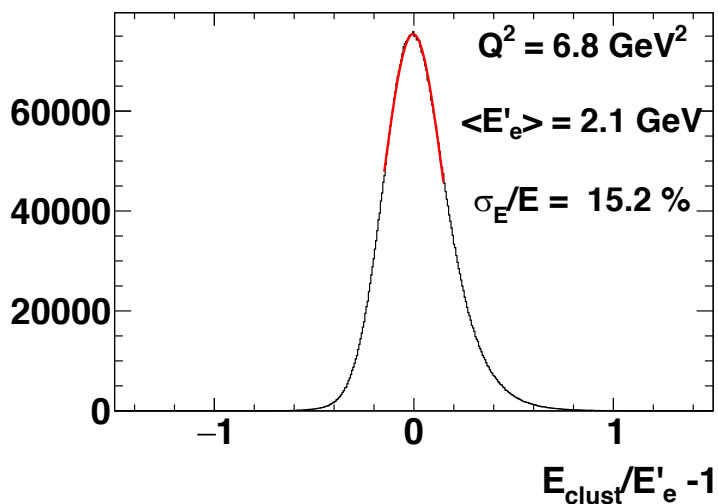
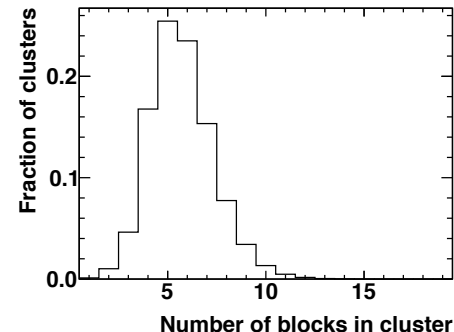
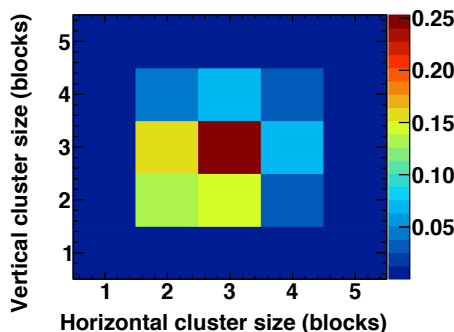
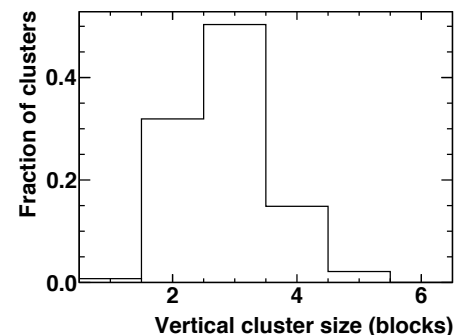
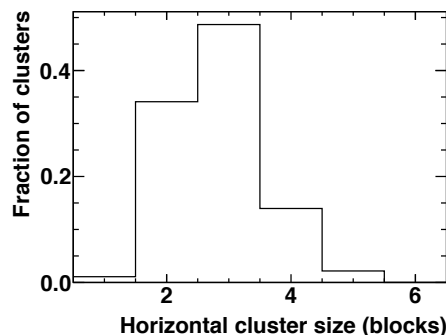
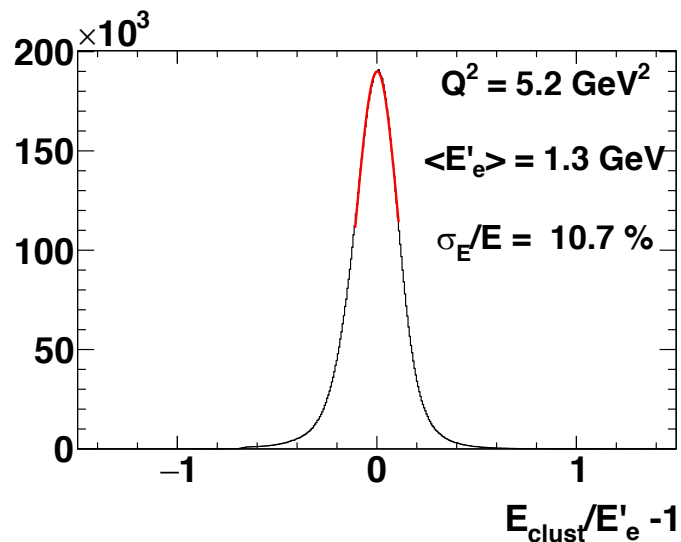


- Alignment strategy: determine best geometric alignment parameters (position, orientation)
- Remove residual spurious correlations via *ad hoc* corrections to FPP track expanded up to 2<sup>nd</sup> order in *HMS* track parameters
- Left: FPP-HMS track parameter differences from straight-through data, before (red-dashed) and after (black solid) applying *ad hoc* alignment corrections
- Right: residual correlation between  $\Delta y'$  and  $x_{HMS}$  removed by *ad hoc* corrections



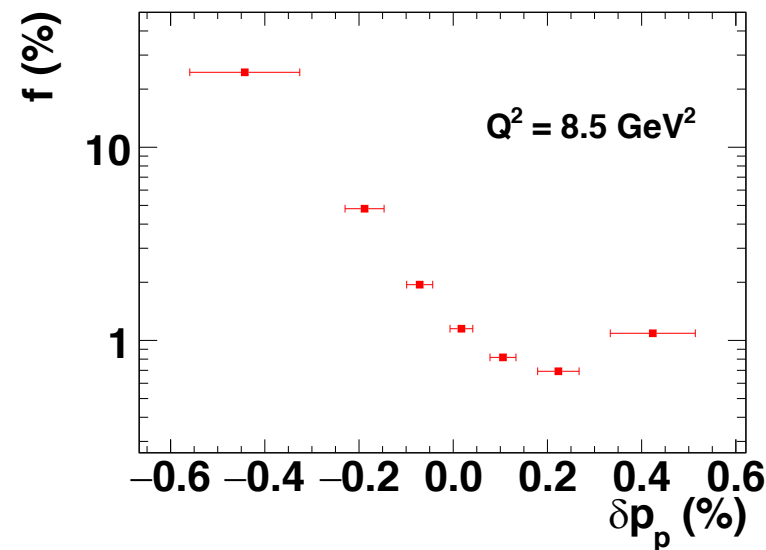
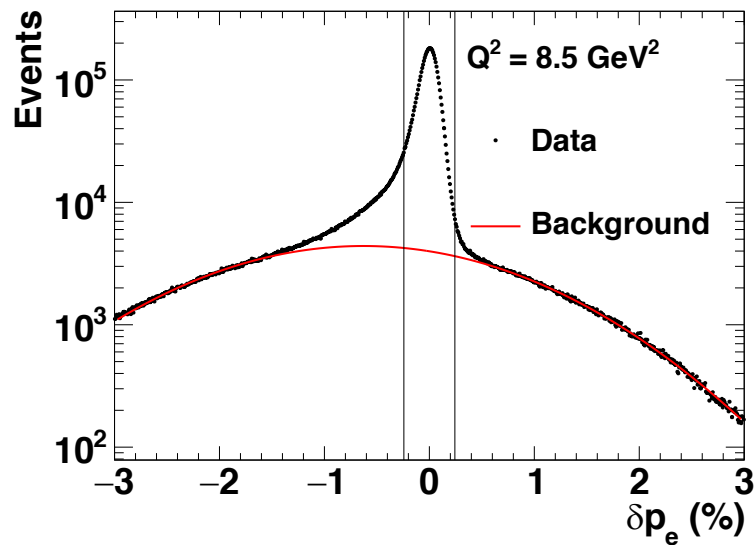
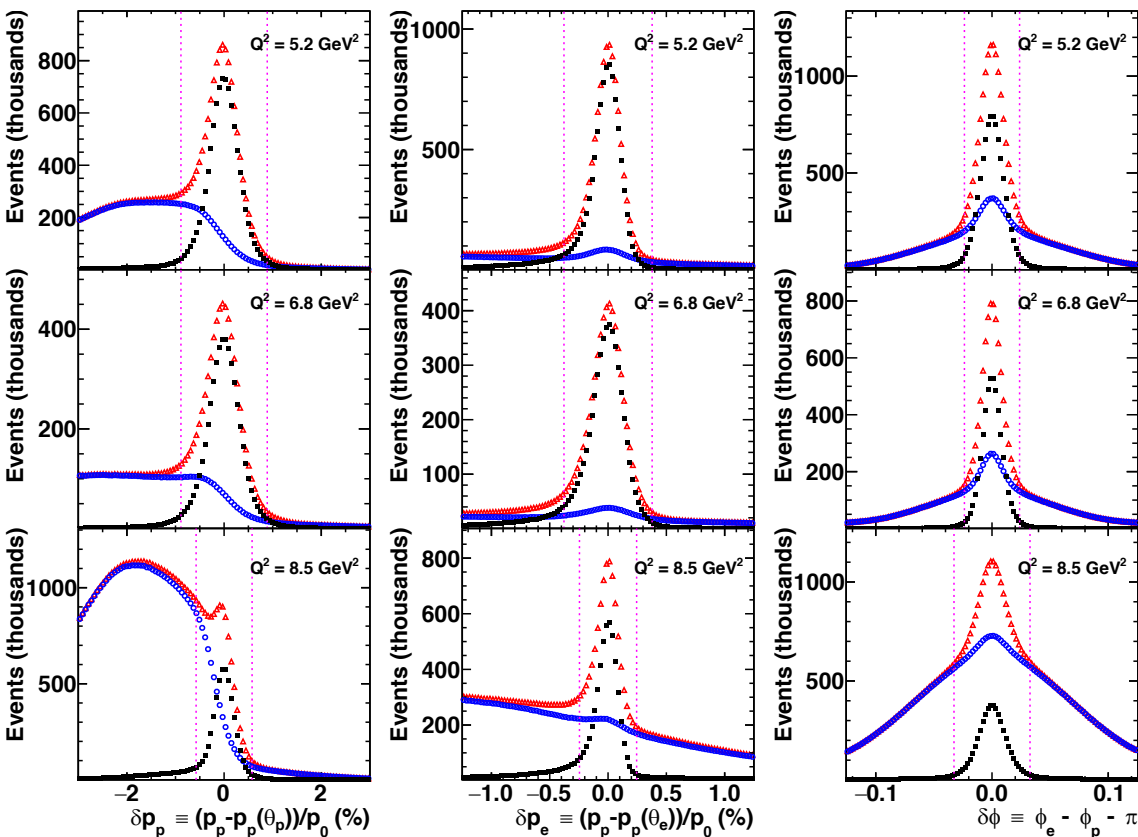
$$\Delta u = C_0^{(u)} + C_x^{(u)}x + C_y^{(u)}y + C_{x'}^{(u)}x' + C_{y'}^{(u)}y' + C_{xx}^{(u)}x^2 + C_{xy}^{(u)}xy + C_{xx'}^{(u)}xx' + C_{xy'}^{(u)}xy' + C_{yy}^{(u)}y^2 + C_{yx'}^{(u)}yx' + C_{yy'}^{(u)}yy' + C_{x'x}^{(u)}x'^2 + C_{x'y'}^{(u)}x'y', \quad (20)$$

# BigCal Reconstruction



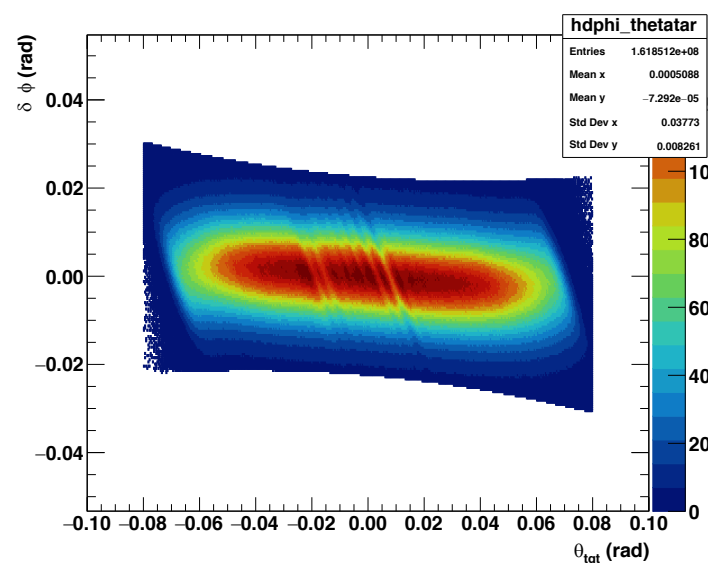
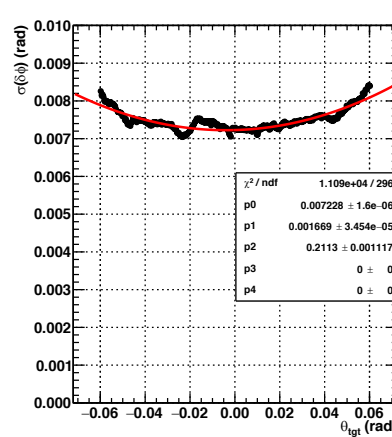
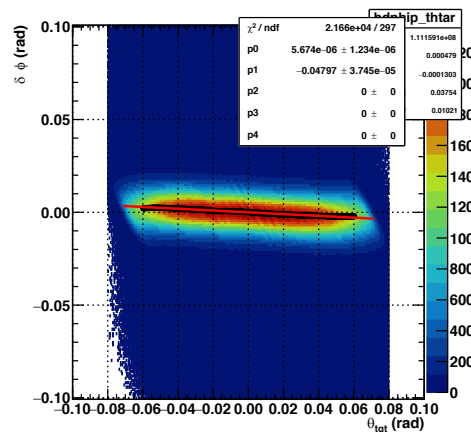
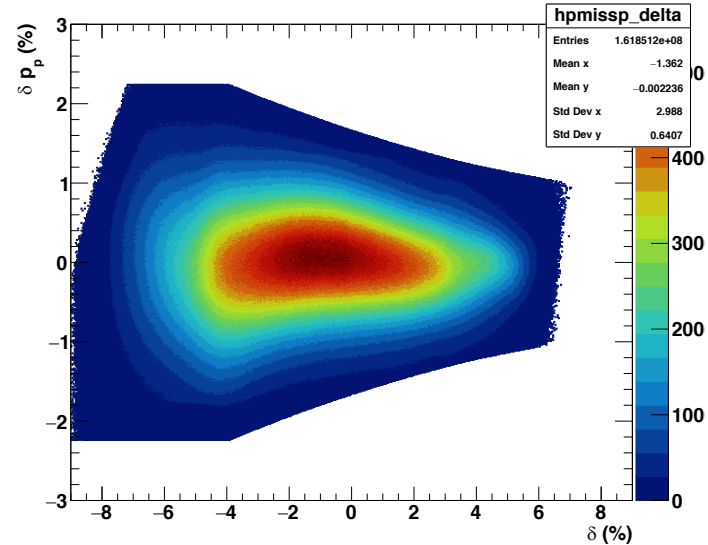
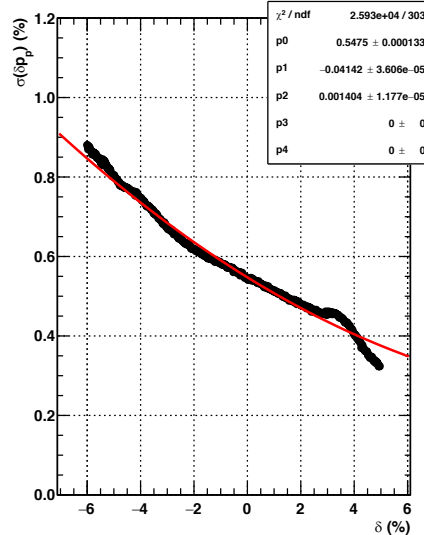
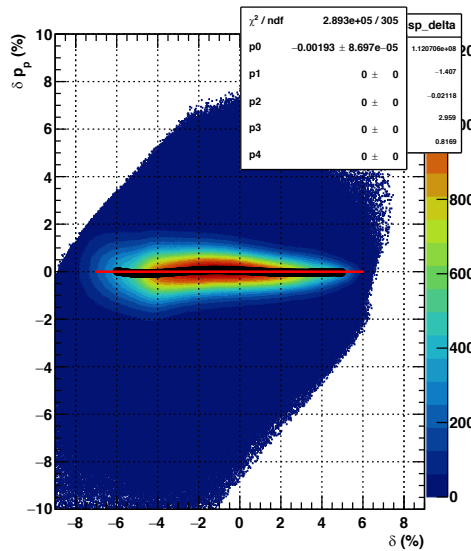
- Left: Energy resolution near beginning of experiment ( $Q^2 = 5.2 \text{ GeV}^2$ ) and end of experiment ( $Q^2 = 6.8 \text{ GeV}^2$ ). Scaled energy resolution at 1 GeV increased from 12%  $\rightarrow$  22% as a result of radiation damage
- Above: BigCal cluster size distribution at  $E' \sim 1.5 \text{ GeV}$

# Elastic Event Selection, I



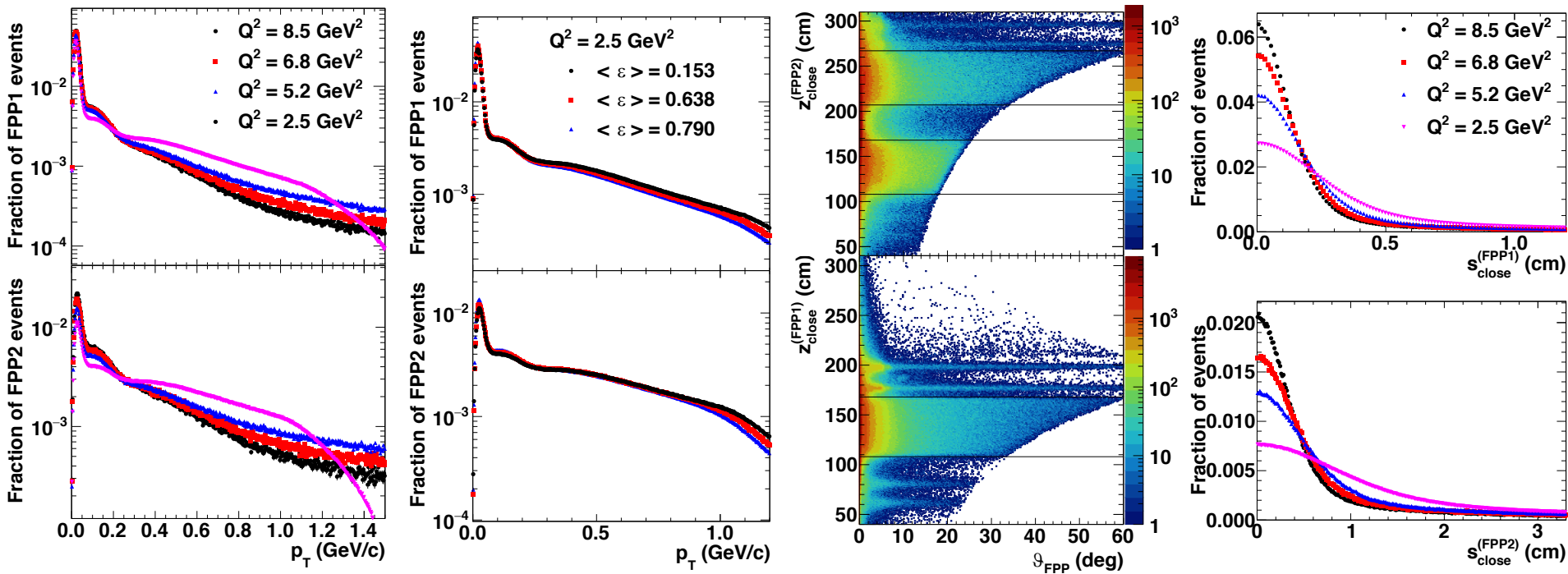
- Above: simplified picture of elastic event selection with fixed-width cuts for GEP-III kinematics
- Right, top: background estimation from sideband analysis of  $\delta p_e$  spectrum
- Right, bottom: estimated fractional background contamination vs.  $\delta p_p$  at  $Q^2 = 8.5 \text{ GeV}^2$

# Elastic Event Selection, II



- Variable-width exclusivity cuts in  $\delta p_p$  and  $\delta \phi$  improve efficiency and signal/background ratio of elastic event selection; and minimize cut-induced bias in the spin transport calculation

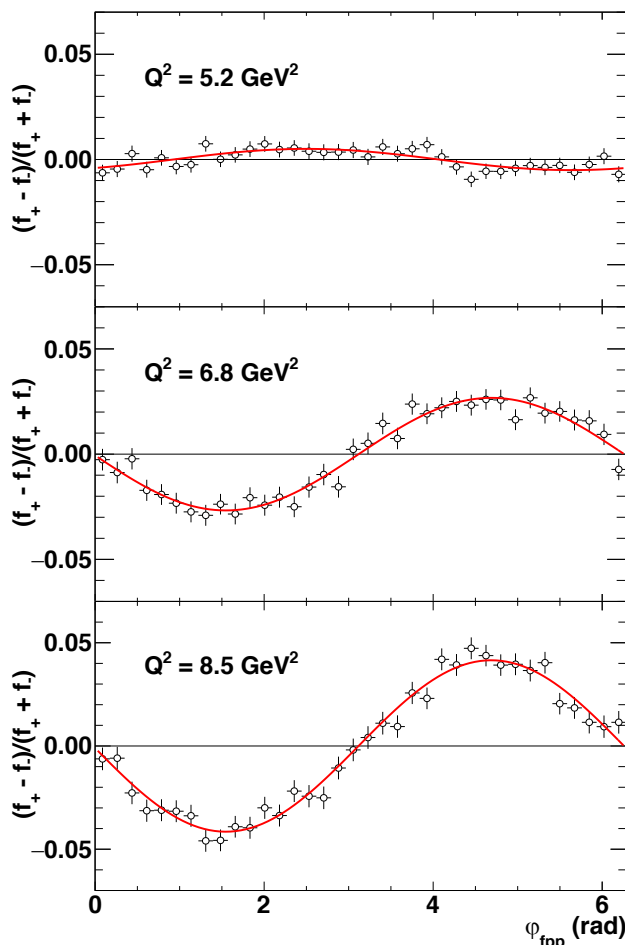
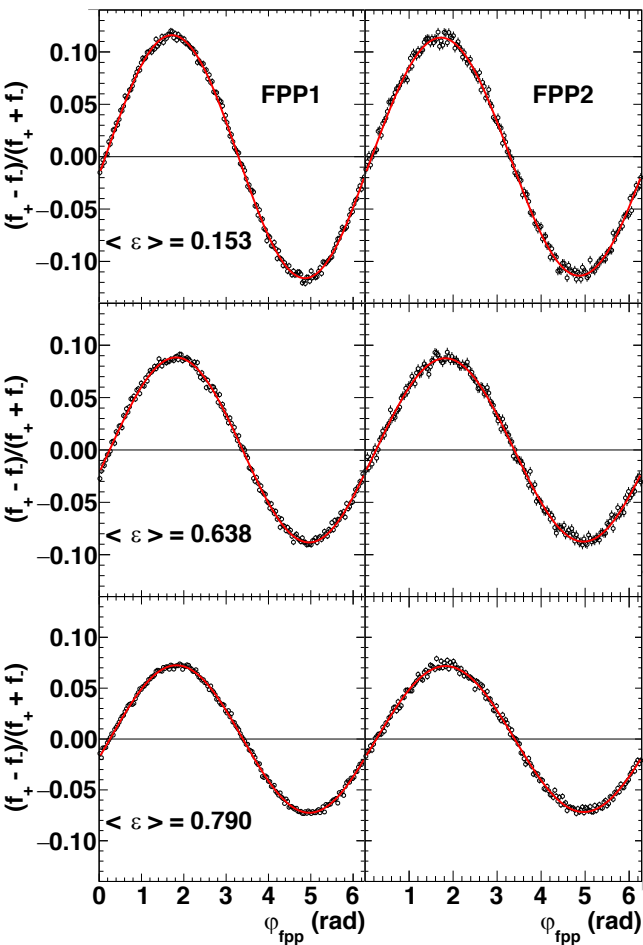
# FPP angular distributions, I



- Far left:  $p_T = p \sin(\theta)$  for different  $Q^2$ , single-track events passing  $s_{\text{close}}$ ,  $z_{\text{close}}$  cuts (closest-approach parameters) and cone test
- Mid left:  $p_T = p \sin(\theta)$  for different  $\epsilon$ ,  $Q^2 = 2.5 \text{ GeV}^2$ , single-track events passing  $s_{\text{close}}$ ,  $z_{\text{close}}$  cuts (closest-approach parameters) and cone test
- Mid right:  $z_{\text{close}}$  vs.  $\theta$  for FPP1 and FPP2,  $Q^2 = 8.5 \text{ GeV}^2$ , single-track events passing  $s_{\text{close}}$  cut and cone test
- Far right:  $s_{\text{close}}$  (distance of closest approach) vs  $Q^2$



# FPP angular distributions, II



$$f^+ - f^- \equiv \frac{\pi}{\Delta\varphi} \left[ \frac{N^+(\varphi)}{N_0^+} - \frac{N^-(\varphi)}{N_0^-} \right] = \bar{A}_y [P_{y,tr}^{FPP} \cos \varphi - P_{x,tr}^{FPP} \sin \varphi] \times [1 + \mu_0(\varphi)] \quad (24)$$

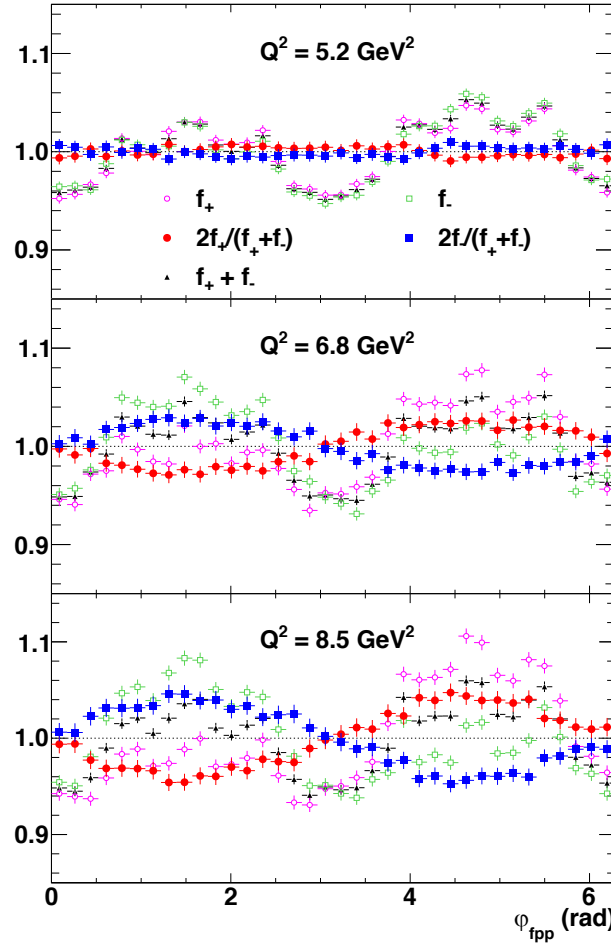
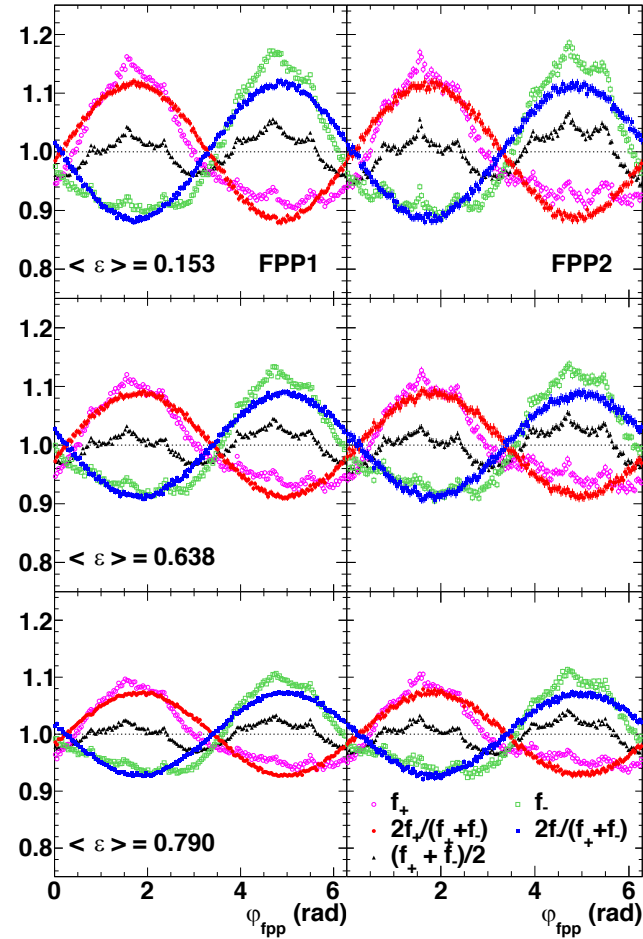
$$f^+ + f^- \equiv \frac{\pi}{\Delta\varphi} \left[ \frac{N^+(\varphi)}{N_0^+} + \frac{N^-(\varphi)}{N_0^-} \right] = [1 + \mu_0(\varphi)] \times [1 + \bar{A}_y (P_{y,ind}^{FPP} \cos \varphi - P_{x,ind}^{FPP} \sin \varphi)] \approx 1 + \mu_0(\varphi) \quad (25)$$

$$\frac{f_+ - f_-}{f_+ + f_-} = \frac{\bar{A}_y (P_{y,tr}^{FPP} \cos \varphi - P_{x,tr}^{FPP} \sin \varphi)}{1 + \bar{A}_y (P_{y,ind}^{FPP} \cos \varphi - P_{x,ind}^{FPP} \sin \varphi)} \approx \bar{A}_y (P_{y,tr}^{FPP} \cos \varphi - P_{x,tr}^{FPP} \sin \varphi) \quad (26)$$

$$\frac{2f_{\pm}}{f_+ + f_-} = 1 \pm \frac{\bar{A}_y (P_{y,tr}^{FPP} \cos \varphi - P_{x,tr}^{FPP} \sin \varphi)}{1 + \bar{A}_y (P_{y,ind}^{FPP} \cos \varphi - P_{x,ind}^{FPP} \sin \varphi)} \approx 1 \pm \bar{A}_y (P_{y,tr}^{FPP} \cos \varphi - P_{x,tr}^{FPP} \sin \varphi) \quad (27)$$

- Left: azimuthal helicity-difference/sum ratio asymmetry for FPP1 and FPP2 for GEp-2gamma kinematics
- Middle: Same for GEp-III kinematics
- Right: Equations for angular distributions in terms of transferred/induced polarizations and false asymmetries

# FPP angular distributions, III



$$f^+ - f^- \equiv \frac{\pi}{\Delta\varphi} \left[ \frac{N^+(\varphi)}{N_0^+} - \frac{N^-(\varphi)}{N_0^-} \right] \\ = \bar{A}_y [P_{y,tr}^{FPP} \cos\varphi - P_{x,tr}^{FPP} \sin\varphi] \times [1 + \mu_0(\varphi)] \quad (24)$$

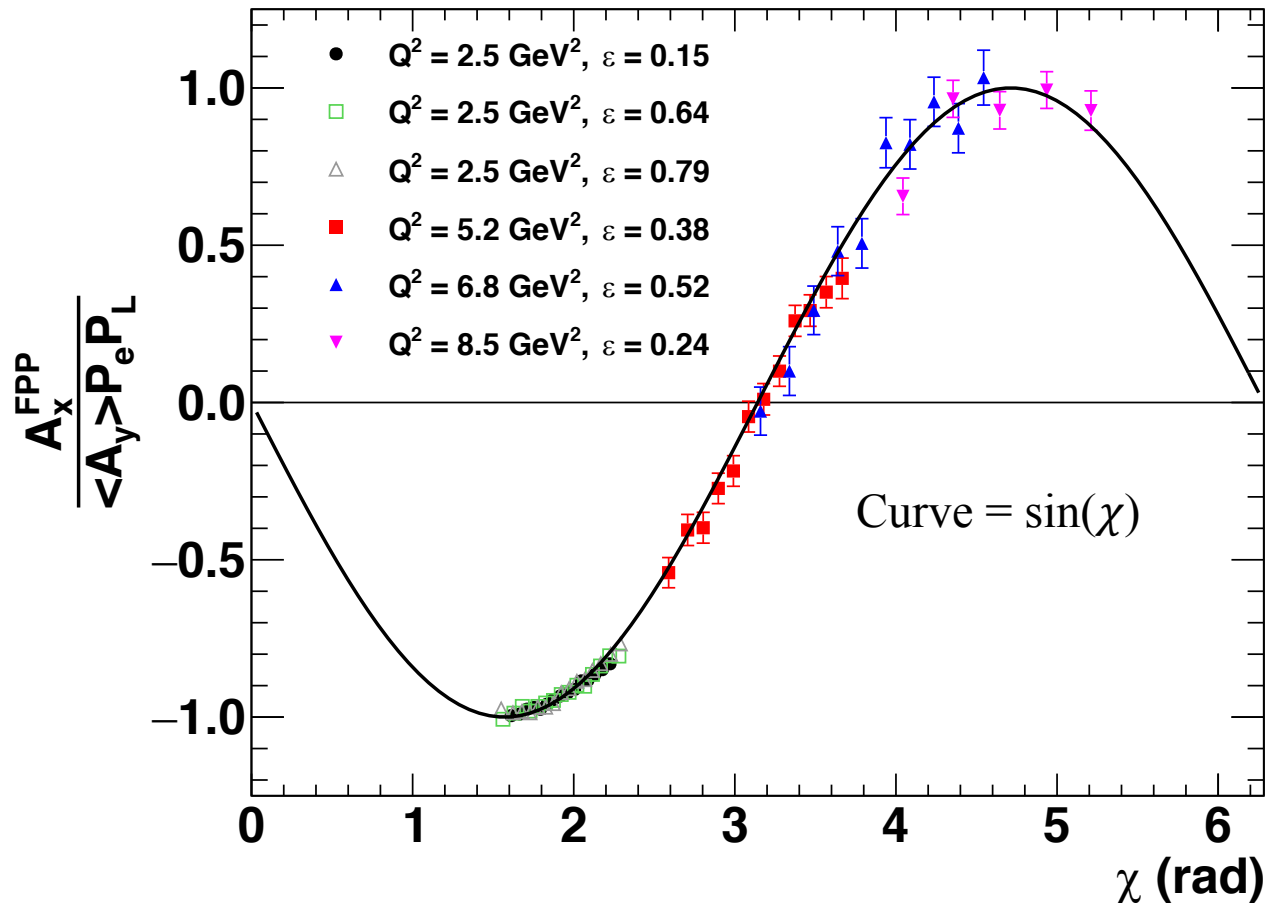
$$f^+ + f^- \equiv \frac{\pi}{\Delta\varphi} \left[ \frac{N^+(\varphi)}{N_0^+} + \frac{N^-(\varphi)}{N_0^-} \right] \\ = [1 + \mu_0(\varphi)] \times [1 + \bar{A}_y (P_{y,ind}^{FPP} \cos\varphi - P_{x,ind}^{FPP} \sin\varphi)] \\ \approx 1 + \mu_0(\varphi) \quad (25)$$

$$\frac{f_+ - f_-}{f_+ + f_-} = \frac{\bar{A}_y (P_{y,tr}^{FPP} \cos\varphi - P_{x,tr}^{FPP} \sin\varphi)}{1 + \bar{A}_y (P_{y,ind}^{FPP} \cos\varphi - P_{x,ind}^{FPP} \sin\varphi)} \\ \approx \bar{A}_y (P_{y,tr}^{FPP} \cos\varphi - P_{x,tr}^{FPP} \sin\varphi) \quad (26)$$

$$\frac{2f_{\pm}}{f_+ + f_-} = 1 \pm \frac{\bar{A}_y (P_{y,tr}^{FPP} \cos\varphi - P_{x,tr}^{FPP} \sin\varphi)}{1 + \bar{A}_y (P_{y,ind}^{FPP} \cos\varphi - P_{x,ind}^{FPP} \sin\varphi)} \\ \approx 1 \pm \bar{A}_y (P_{y,tr}^{FPP} \cos\varphi - P_{x,tr}^{FPP} \sin\varphi) \quad (27)$$

- Left: azimuthal angle distributions for +,- helicities, their sum and their ratio to the sum, vs  $\varepsilon$  at  $Q^2 = 2.5$   $\text{GeV}^2$
- Mid: Same for GEp-III kinematics
- Right: Equations for angular distributions in terms of transferred/induced polarizations and false asymmetries

# Spin Precession



- Large acceptance of the HMS in the main “dipole” precession angle  $\chi$  and generally large values of  $P_L$  means that even with a central precession angle near 180 deg., the uncertainty in  $R$  is dominated by the determination of  $P_T$ ; even at  $Q^2 = 5.2$ ,  $\Delta P_T/P_T \sim 4\Delta P_L/P_L$

# Analyzing Power Calibration

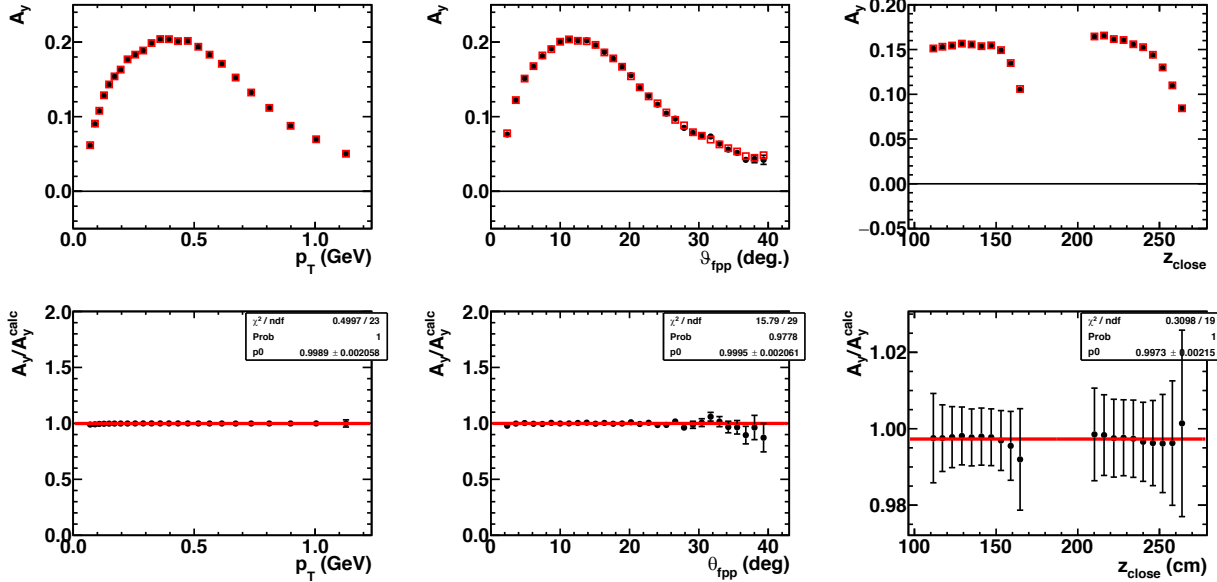
$$\hat{P}_t^{(A_y=1)} = \bar{A}_y P_t$$

$$\hat{P}_\ell^{(A_y=1)} = \bar{A}_y P_\ell$$

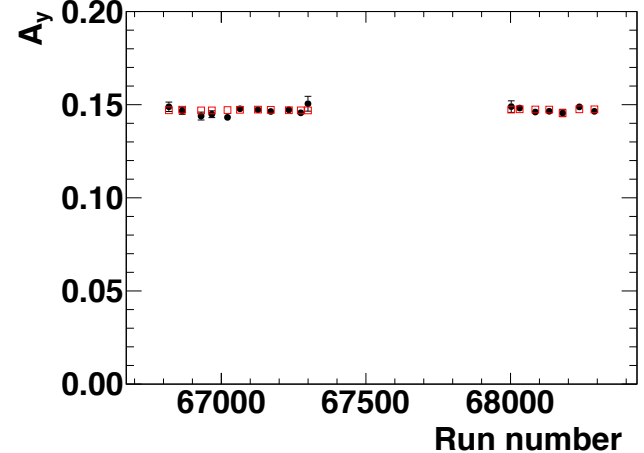
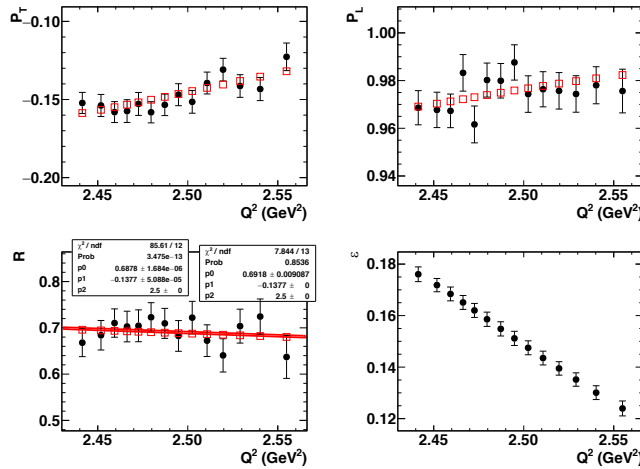
$$\bar{A}_y = \frac{\hat{P}_t^{(A_y=1)}}{P_t^{Born}} = \frac{\hat{P}_\ell^{(A_y=1)}}{P_\ell^{Born}}$$

$$P_t^{Born} = -\sqrt{\frac{2\epsilon(1-\epsilon)}{\tau}} \frac{r}{1 + \frac{\epsilon}{\tau} r^2}$$

$$P_\ell^{Born} = \frac{\sqrt{1-\epsilon^2}}{1 + \frac{\epsilon}{\tau} r^2}$$

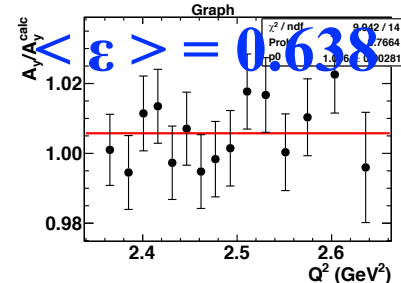
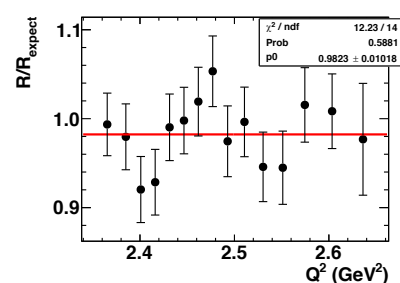
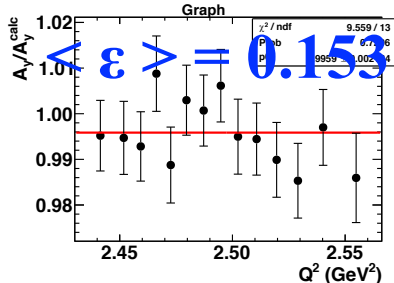
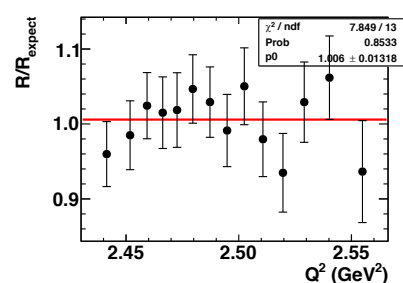
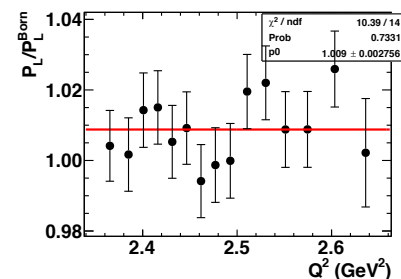
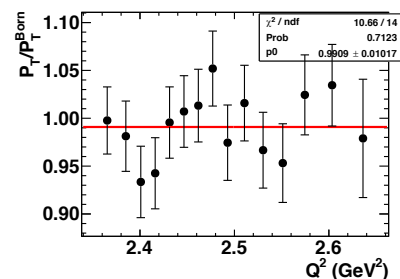
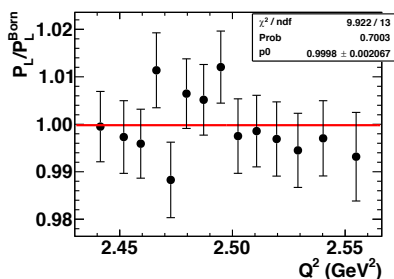
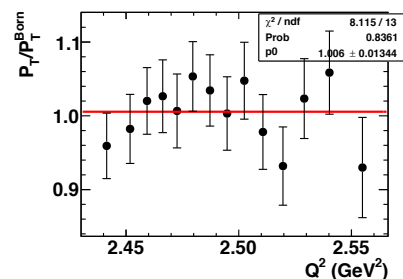


- Analyzing power for  $Q^2 = 2.5$   $\text{GeV}^2$  is calibrated using the low- $\epsilon$  point:
  - $P_L^{Born}$  is very insensitive to the FF ratio at this ( $\epsilon$ ,  $Q^2$ )
- 2D binning in  $p_T = p \sin(\theta)$  and  $z_{close}$
- Momentum dependence accounted for using an overall  $1/p$  scaling event-by-event

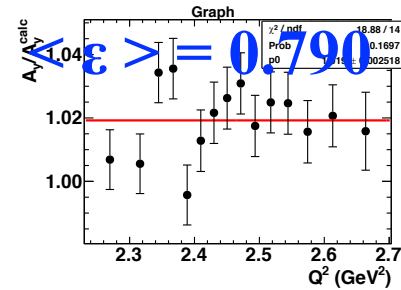
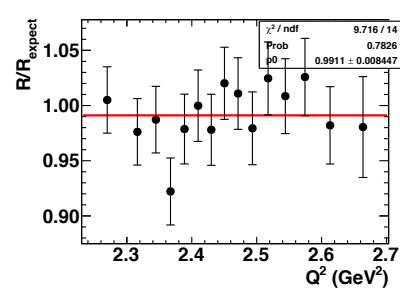
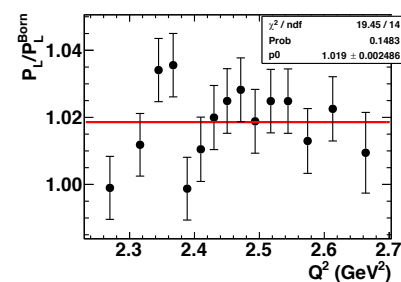
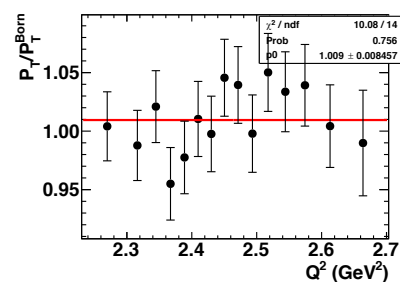


**Key assumption for full acceptance extraction of  $P_L/P_L^{Born}$ :  $p_T$  dependence of  $A_y$  factorizes from  $p_p$  dependence:  $A_y = A_y^0(p_T)/p$**

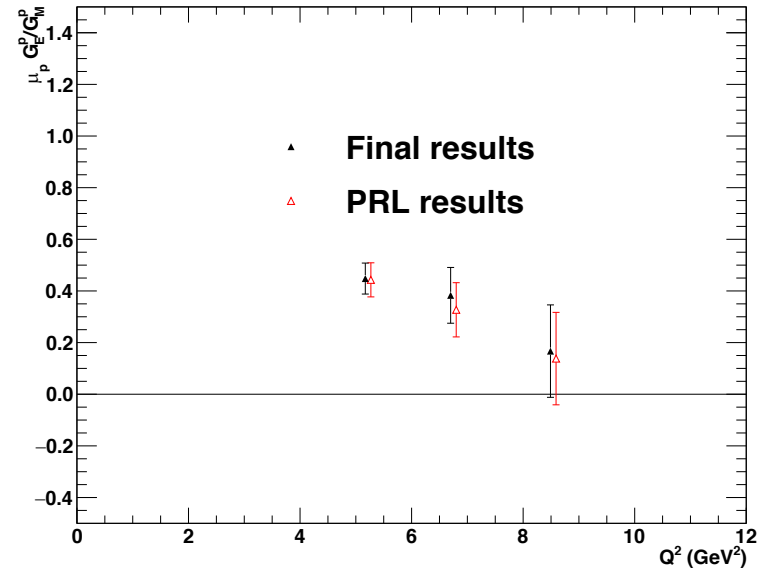
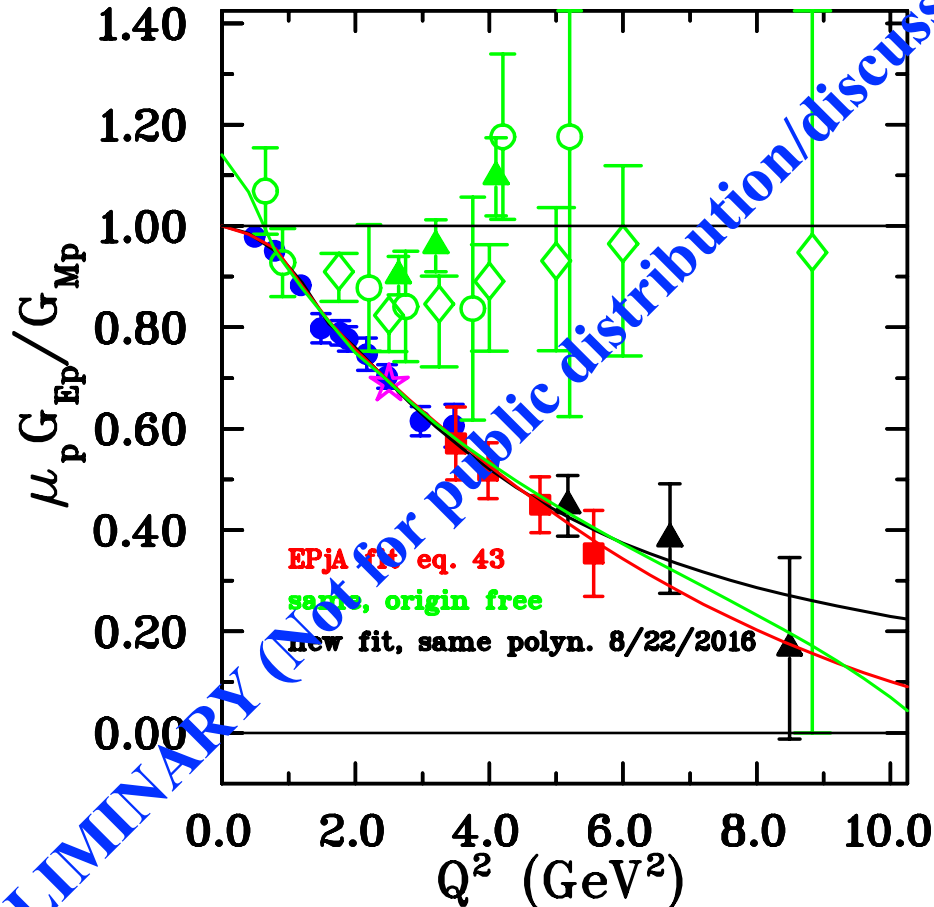
# Checking the momentum scaling of $A_y$



- Crucial for  $P_L/P_L^{\text{Born}}$  extraction is the application of the same cuts on all parameters of the secondary scattering ( $p_T$ ,  $s_{\text{close}}$ ,  $z_{\text{close}}$ ) and the event topology (single-track events passing cone test); the effective average  $A_y$  should be the same up to the momentum dependence and the different  $Q^2/p_p$  ranges accepted by the HMS for different  $\epsilon$  values
- Same central momentum setting also insures that the spin precession is the same and the associated p.t.p. systematics are very small.



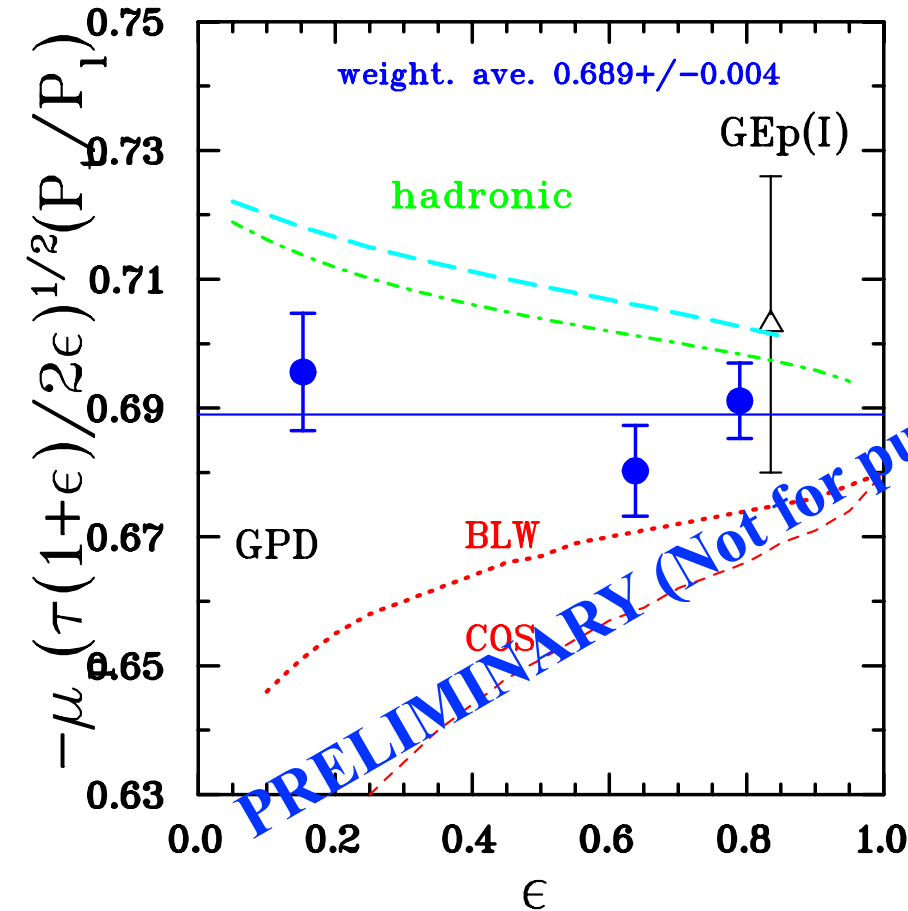
# GEP-III Final Archival Results (PRELIMINARY)



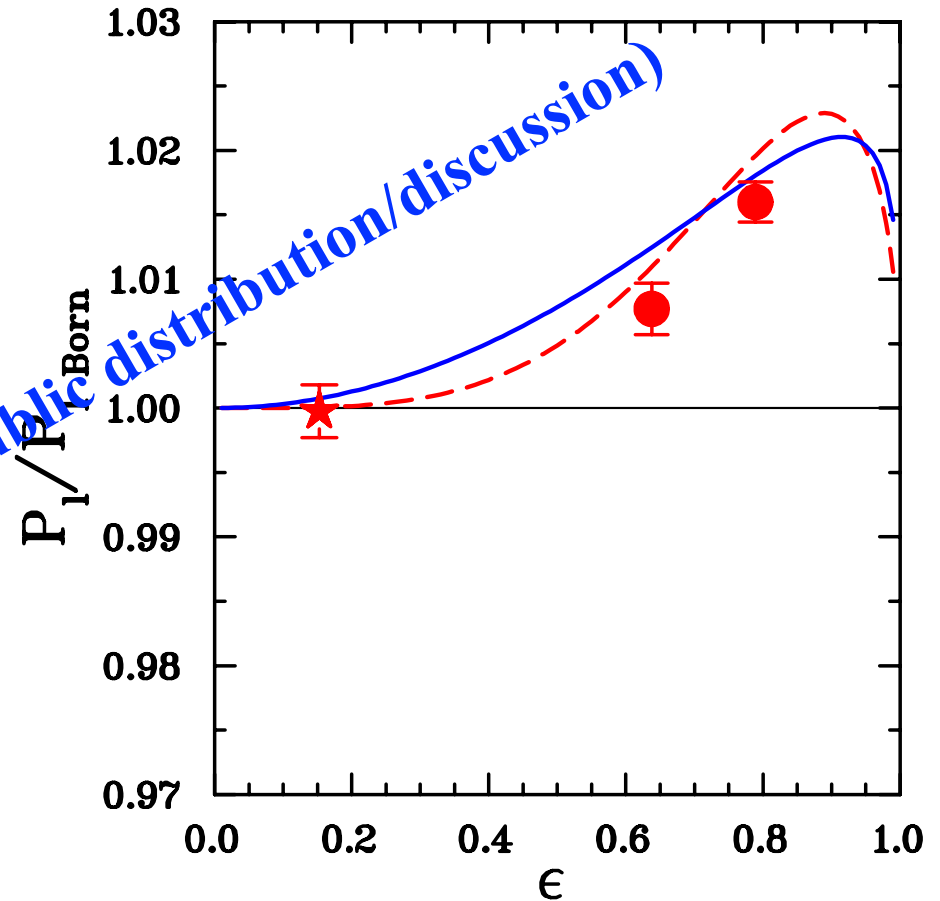
- GEP-III final results:
  - Statistically and systematically insignificant increases at  $Q^2 = 6.8, 8.5 \text{ GeV}^2$  relative to original publication.  $5.2 \text{ GeV}^2$  result virtually identical
  - Statistical error reduced from 0.066  $\rightarrow$  0.060 at  $5.2 \text{ GeV}^2$ , reflecting the (previously neglected) covariance term between  $P_T, P_L$

report allpol alles GEP3PRC 07122016 08/22/16

# GEP-2gamma Final Archival Results (PRELIMINARY)



twogamma toppanel 01282015 7/16/16



twogamma bot GEPSPRC 1/5/17

- **Final analysis of GEP-2gamma with full-acceptance data more than doubles statistics at  $\epsilon = 0.638, 0.790$**
- Only stat. errors are shown here
- Our conclusions with respect to R and  $P_L/P_L^{\text{Born}}$  are basically unchanged, although the enhancement of  $P_L$  at large  $\epsilon$  is somewhat smaller (but consistent to within stat. and syst. errors with original PRL publication, which only included data within an artificially restricted acceptance matched to the lowest  $\epsilon$ )

# Status, Summary and Conclusions

Polarization Transfer Observables in Elastic Electron-Proton Scattering at  $Q^2 = 2.5, 5.2, 6.8$  and  $8.5 \text{ GeV}^2$

A. J. R. Puckett,<sup>1,2,\*</sup> E. J. Brash,<sup>3,4</sup> M. K. Jones,<sup>4</sup> W. Luo,<sup>5</sup> M. Meziane,<sup>6</sup> L. Pentchev,<sup>6</sup> C. F. Perdrisat,<sup>6</sup> V. Punjabi,<sup>7</sup> F. R. Wesselmann,<sup>7</sup> A. Ahmidouch,<sup>8</sup> I. Albayrak,<sup>9</sup> K. A. Aniol,<sup>10</sup> J. Arrington,<sup>11</sup> A. Asaturyan,<sup>12</sup> H. Baghdasaryan,<sup>13</sup> F. Benmokhtar,<sup>14</sup> W. Bertozzi,<sup>1</sup> L. Bimbot,<sup>15</sup> P. Bosted,<sup>4</sup> W. Boeglin,<sup>16</sup> C. Butuceanu,<sup>17</sup> P. Carter,<sup>3</sup> S. Chernenko,<sup>18</sup> E. Christy,<sup>9</sup> M. Commisso,<sup>13</sup> J. C. Cornejo,<sup>10</sup> S. Covrig,<sup>4</sup> S. Danagoulian,<sup>8</sup> A. Daniel,<sup>19</sup> A. Davidenko,<sup>20</sup> D. Day,<sup>13</sup> S. Dhamija,<sup>16</sup> D. Dutta,<sup>21</sup> R. Ent,<sup>4</sup> S. Frullani,<sup>22</sup> H. Fenker,<sup>4</sup> E. Fries,<sup>13</sup> F. Garibaldi,<sup>22</sup> D. Gaskell,<sup>4</sup> S. Gilad,<sup>1</sup> R. Gilman,<sup>4,23</sup> Y. Goncharenko,<sup>20</sup> K. Hafidi,<sup>11</sup> D. Hamilton,<sup>24</sup> D. W. Higinbotham,<sup>4</sup> W. Hinton,<sup>7</sup> T. Horn,<sup>4</sup> B. Hu,<sup>5</sup> J. Huang,<sup>1</sup> G. M. Huber,<sup>17</sup> E. Jensen,<sup>3</sup> C. Keppel,<sup>9</sup> M. Khandaker,<sup>7</sup> P. King,<sup>19</sup> D. Kirillov,<sup>18</sup> M. Kohl,<sup>9</sup> V. Kravtsov,<sup>20</sup> G. Kumbartzki,<sup>23</sup> Y. Li,<sup>9</sup> V. Mamyán,<sup>13</sup> D. J. Margaziotis,<sup>10</sup> A. Marsh,<sup>3</sup> Y. Matulenko,<sup>20</sup> J. Maxwell,<sup>13</sup> G. Mbianda,<sup>25</sup> D. Meekins,<sup>4</sup> Y. Melnik,<sup>20</sup> J. Miller,<sup>26</sup> A. Mkrtychyan,<sup>12</sup> H. Mkrtychyan,<sup>12</sup> B. Moffit,<sup>1</sup> O. Moreno,<sup>10</sup> J. Mulholland,<sup>13</sup> A. Narayan,<sup>21</sup> S. Nedev,<sup>27</sup> Nuruzzaman,<sup>21</sup> E. Piasetzky,<sup>28</sup> W. Pierce,<sup>3</sup> N. M. Piskunov,<sup>18</sup> Y. Prok,<sup>3</sup> R. D. Ransome,<sup>23</sup> D. S. Razin,<sup>18</sup> P. Reimer,<sup>11</sup> J. Reinhold,<sup>16</sup> O. Rondón,<sup>13</sup> M. Shabestari,<sup>13</sup> A. Shahinyan,<sup>12</sup> K. Shestermanov,<sup>20,†</sup> S. Širca,<sup>29</sup> I. Sitnik,<sup>18</sup> L. Smykov,<sup>18,†</sup> G. Smith,<sup>4</sup> L. Solovyev,<sup>20</sup> P. Solvignon,<sup>11</sup> R. Subedi,<sup>13</sup> E. Tomasi-Gustafsson,<sup>15,30</sup> A. Vasiliev,<sup>20</sup> M. Veilleux,<sup>3</sup> B. B. Wojtsekhowski,<sup>4</sup> S. Wood,<sup>4</sup> Z. Ye,<sup>9</sup> Y. Zanevsky,<sup>18</sup> X. Zhang,<sup>5</sup> Y. Zhang,<sup>5</sup> X. Zheng,<sup>13</sup> and L. Zhu<sup>1</sup>

<sup>1</sup>Massachusetts Institute of Technology, Cambridge, MA 02139

<sup>2</sup>University of Connecticut, Storrs, CT 06269

<sup>3</sup>Christopher Newport University, Newport News, VA 23606

<sup>4</sup>Thomas Jefferson National Accelerator Facility, Newport News, VA 23606

<sup>5</sup>Lanzhou University, Lanzhou 730000, Gansu, Peoples Republic of China

<sup>6</sup>College of William and Mary, Williamsburg, VA 23187

<sup>7</sup>Norfolk State University, Norfolk, VA 23504

<sup>8</sup>North Carolina A&T State University, Greensboro, NC 27411

<sup>9</sup>Hampton University, Hampton, VA 23668

<sup>10</sup>California State University Los Angeles, Los Angeles, CA 90032

<sup>11</sup>Argonne National Laboratory, Argonne, IL, 60439

<sup>12</sup>Yerevan Physics Institute, Yerevan 375036, Armenia

<sup>13</sup>University of Virginia, Charlottesville, VA 22904

<sup>14</sup>Carnegie Mellon University, Pittsburgh, PA 15213

<sup>15</sup>Institut de Physique Nucléaire, CNRS/IN2P3 and Université Paris-Sud, France

<sup>16</sup>Florida International University, Miami, FL 33199

<sup>17</sup>University of Regina, Regina, SK S4S 0A2, Canada

<sup>18</sup>JINR-LHE, Dubna, Moscow Region, Russia 141980

<sup>19</sup>Ohio University, Athens, Ohio 45701

<sup>20</sup>JHEP, Protvino, Moscow Region, Russia 142284

<sup>21</sup>Mississippi State University, Mississippi, MS 39762

<sup>22</sup>INFN, Sezione Sanità and Istituto Superiore di Sanità, 00161 Rome, Italy

<sup>23</sup>Rutgers, The State University of New Jersey, Piscataway, NJ 08855

<sup>24</sup>University of Glasgow, Glasgow G12 8QQ, Scotland UK

<sup>25</sup>University of Witwatersrand, Johannesburg, South Africa

<sup>26</sup>University of Maryland, College Park, MD 20742

<sup>27</sup>University of Chemical Technology and Metallurgy, Sofia, Bulgaria

<sup>28</sup>University of Tel Aviv, Tel Aviv, Israel

<sup>29</sup>University of Ljubljana, SI-1000 Ljubljana, Slovenia

<sup>30</sup>DSM, IRFU, SPhN, Saclay, 91191 Gif-sur-Yvette, France

This is the abstract of our paper.

## I. INTRODUCTION

Scattering of electrons or of real photons is of great importance for the characterization of the structure of the

nucleon as well as nuclei, because of the relative weakness of the electromagnetic interaction, compared to that of strongly interacting probes like nucleons or mesons. The field of elastic electron scattering received its initial start with the availability of electron beams of several hundreds of MeV (up to 550 MeV) at the High Energy Physics Laboratory (HEPL) in Stanford in the middle 1950's. One particularly outstanding result was the determination of a proton radius [1], which together with

\* Corresponding author: puckett@jlab.org

† Deceased.